Investigation of the oxohalogenide $Cu_4Te_5O_{12}Cl_4$ with weakly coupled Cu(II) tetrahedra

Rie Takagi[a], Mats Johnsson[a], Vladimir Gnezdilov[b], Reinhard K. Kremer[c], Wolfram Brenig[d], and Peter Lemmens[c,e]
[a] *Department of Inorganic Chemistry, Stockholm University, S-106 91 Stockholm, Sweden*
[b] *B. I. Verkin Institute for Low Temperature Physics NASU, 61164 Kharkov, Ukraine*
[c] *Max Planck Institute for Solid State Research, Heisenbergstrasse 1, D-70569 Stuttgart, Germany*
[d] *Institute for Theoretical Physics, TU Braunschweig, D-38106 Braunschweig, Germany*
[e] *Institute for Physics of Condensed Matter, TU Braunschweig, D-38106 Braunschweig, Germany*
(Dated: February 5, 2008)

The crystal structure of the copper(II) tellurium(IV) oxochloride $Cu_4Te_5O_{12}Cl_4$ (Cu-45124) is composed of weakly coupled tetrahedral Cu clusters and shows crystallographic similarities with the intensively investigated compound $Cu_2Te_2O_5X_2$, with X = Cl, Br (Cu-2252). It differs from the latter by a larger separation of the tetrahedra within the crystallographic *ab* plane, that allows a more direct assignment of important inter-tetrahedra exchange paths and the existence of an inversion center. Magnetic susceptibility and specific heat evidence antiferromagnetic, frustrated correlations of the Cu spin moments and long range ordering with T_c=13.6 K. The entropy related to the transition is reduced due to quantum fluctuations. In Raman scattering a well structured low energy magnetic excitation is observed at energies of ≈50K (35cm^{-1}). This energy scale is reduced as compared to Cu-2252.

PACS numbers: 75.30.-m, 72.80.Ga, 71.30.+h, 65.40.Ba

I. INTRODUCTION

Quantum spin systems are interesting due to strong fluctuation effects, unconventional ground states and a pronounced electronic and magnetic softness. The latter leads to large responses to external fields and changes of composition[1]. Competing exchange interactions in geometrically frustrated, e.g. triangular or tetrahedral lattices, enhance this trend, suppress long range ordering and shift relevant excitations to lower energies. An important aspect of such systems is the coupling of the frustrated entities, e.g. triangles or tetrahedra, to larger units, as planes or framework structures. Quantum criticality and related phenomena can be tuned by favorably modifying the coupling between such units[2,3,4,5]. Strongly coupled, corner sharing tetrahedra exist e.g. in the pyrochlores. These compounds show spin ice states or unconventional transitions into spin liquid phases[6,7,8,9]. The implications of inter-tetrahedra couplings of different strength, dimensionality or topology are intensively studied theoretically, for example in Ref. 10,11,12,13.

The compound $Cu_2Te_2O_5X_2$, X=Br and Cl, (Cu-2252) which contains weakly coupled Cu_4^{2+} tetrahedra is a model system with this respect as the coupling of the Cu tetrahedra can be tuned continuously by varying the stoichiometry[14,15,16]. Cu-2252 shows incommensurate long-range ordering with strongly reduced ordered moments and transition temperatures for X=Br. The ordered magnetic structure is most probably a complex helical structure as demonstrated for X=Cl[17]. Finally, also unconventional collective modes are observed as longitudinal magnons for X=Br in Raman scattering[15,18,19] and a dichotomy of temperature dependent and invariant magnons in neutron scattering[17,20]. The presence of longitudinal magnons has been taken as evidence for the system being close to a quantum critical point[16,18].

Hydrostatic pressure enhances the intra-tetrahedra coupling in both compounds and reduces the inter-tetrahedra coupling for X=Br, respectively, shifting the system closer to the quantum critical point[21,22]. There even exist evidence for a complete suppression of long range order for X=Br[21]. The large response of Cu-2252 on changes of composition and hydrostatic pressure[23] is based on a complex network of exchange paths that are dominated by halogen-mediated exchange in the *ab* plane[24].

The aim of our present study is to extend the number of related systems with unusual magnetic properties. So far, in the phase diagram $CuO : CuX_2$ (X = Cl, Br) : TeO_2 only two compounds have been identified; the previously discussed Cu-2252[14] and a mixed AF/FM dimer chain system $Cu_3(TeO_3)_2Br_2$[25]. The crystal structure of the present system $Cu_4Te_5O_{12}Cl_4$ (Cu-45124) has many similarities with the previously know Cu-2252. Nevertheless, their physical properties are different enough to enable to a better understanding of the properties and phase diagram of weakly coupled tetrahedra systems.

In the following we will describe aspects of the sample preparation of Cu-45124, compare its structural and electronic

properties with those of other Te(IV) electron lone pair systems and investigate its thermodynamic and spectroscopic properties. The relevance of Dzyaloshinsky-Moriya (DM) and spin-phonon interaction will be discussed.

II. EXPERIMENTAL

Single crystals of the compound Cu-45124 were synthesized in sealed evacuated silica tubes. $CuCl_2$ (Avocado Research Chemicals, +98%), CuO (Avocado Research Chemicals, +99%), TeO_2 (ABCR, +99%) were used as starting materials. $CuCl_2$: CuO : TeO_2 were mixed in the stoichiometric molar ratio 2 : 2 : 5 and sealed into evacuated silica tubes (length $\sim$ 6 cm). The tubes were heated at 500 $^\circ$C for 72 h in a box furnace. The product consists of small green bulky non-hygroscopic single crystals. Attempts to synthesize a Br-analogue failed so far. Our experiments gave the previously known compound $Cu_2Te_2O_5Br_2$ in addition to unreacted TeO_2.

Single-crystal X-ray diffraction data were collected on a STOE IPDS image-plate rotating anode diffractometer using graphite-monochromatized Mo Kα radiation, $\lambda = 0.71073$ Å. The intensities of the reflections were integrated with the STOE software and absorption corrections were carried out numerically, after crystal shape optimization[26,27]. The structure was solved by direct methods[28] and refined by full matrix least squares on F^2 (Ref 29). All atoms were refined with anisotropic displacement parameters. The crystallographic data are reported in Table I[30]. The chemical composition was checked in a scanning electron microscope (SEM, JEOL 820) equipped with an energy-dispersive spectrometer (EDS, LINK AN10000).

Monophasic powder of Cu-45124 was checked with X-ray powder diffraction using a Guiner-Hägg focusing camera with subtraction geometry (CuKα_1 radiation, $\lambda = 1.54060$ Å) For the determination of the lattice parameters silicon ($a = 5.43088(4)$ Å) was added as an internal standard. The recorded films were read in with an automatic film scanner and the data were treated using the programs SCANPI and PIRUM. Refinement of the tetragonal unit cell by powder X-ray diffraction resulted in $a = 11.3474(6)$ Å, $c = 6.3439(5)$ Å. The magnetic susceptibility and specific heat data were collected using a SQUID magnetometer (MPMS, Quantum Design) and a Physical Property Measurement System system with specific heat options (PPMS, Quantum Design). For Raman scattering experiments individual single crystals with typical dimensions of approximately 200-300 μm diameter were used with the 514.5 nm excitation line of an Ar^+ Laser and a laser power of P=1 mW in quasi-backscattering geometry. The scattered spectra were collected by a DILOR-XY triple spectrometer and a nitrogen cooled CCD detector with a spectral resolution of approximately 1 cm^{-1}. Due to the transparency and irregular shape of the single crystals the exciting Laser line probes the bulk of the crystal. However, symmetry information of the excitations is lost.

III. CRYSTAL STRUCTURE

The present compound Cu-45124 crystallizes in the tetragonal system, space group $P4/n$[30]. Atomic coordinates and selected angles are listed in the Tables I, II, III and are shown in the Figures 1 and 2. As the chemical and structural peculiarities of this class of compounds are based on Te^{4+} and its lone pair electron we will first discuss the Te coordinations. The interplay of the lone pair electrons on the background of the oxohalide framework is important as it allows voids in the crystal structure and a large electronic polarizability. This shows up, e. g. as a large Raman scattering intensity in Cu-45124. The intra- and inter-tetrahedra exchange paths and exchange couplings that realize weakly coupled tetrahedra are dominated by Cu–O and Cu–Cl coordinations and will be discussed later.

TABLE I: Crystal data for Cu-45124 at T=298 K[30].

Empirical formula	$Cu_4Te_5O_{12}Cl_4$
Formula weight	1225.96 g/mol
Crystal system, Space group	Tetragonal, P 4/n
Unit cell dimensions	$a = 11.3474(16)$ Å $c = 6.3319(9)$ Å
Volume	815.3(2) Å^3
Z	2
Density (calculated)	4.994 g/cm^3

The Te(2) atom has a see-saw [TeO_{3+1}] coordination with three Te – O bond distances in the range 1.870 – 1.930 Å, the fourth long Te(2) – O(3) distance amounts to 2.499 Å. There is a fifth long Te(2) – O(1) distance with

TABLE II: Atomic coordinates for Cu-45124. All atoms are refined with anisotropic displacement parameters, however, only the isotropic displacement parameters are shown in the table. U(eq) is defined as one-third of the trace of the orthogonalized U tensor. BVS is the bond valence sum calculated using parameters from Refs. 31,34.

Atom	**Wyck.**	**x**	**y**	**z**	**U_{eq} [Å^2]**	**BVS**
Te(1)	2c	1/4	1/4	0.3682(3)	0.0117(3)	3.89
Te(2)	8g	0.67623(5)	0.02031(5)	0.86708(11)	0.0075(2)	3.87
Cu	8g	0.75930(11)	0.40494(10)	0.3481(2)	0.0110(3)	2.06
Cl	8g	0.8874(3)	0.5554(2)	0.3341(5)	0.0225(7)	0.52
O(1)	8g	0.2867(6)	0.4044(6)	0.2355(12)	0.0138(17)	2.13
O(2)	8g	0.2848(5)	0.8712(6)	0.3558(12)	0.0098(15)	2.17
O(3)	8g	0.2876(6)	0.5764(6)	0.9397(11)	0.0100(15)	2.11

TABLE III: Selected bond angles ($^\circ$) for Cu-45124.

O(1)—Te(1)—O(1)×4	79.69(18)	$O(3)^{v}$—Cu—$O(2)^{vi}$	171.1(3)
O(1)—Te(1)—O(1)×2	130.0(5)	$O(3)^{v}$—Cu—$O(2)^{vii}$	83.9(3)
$O(3)^{iv}$—Te(2)—$O(2)^{v}$	96.1(3)	$O(2)^{vi}$—Cu—$O(2)^{vii}$	87.3(3)
$O(3)^{iv}$—Te(2)—$O(1)^{vi}$	90.7(3)	$O(3)^{v}$—Cu—Cl	93.3(2)
$O(2)^{v}$—Te(2)—$O(1)^{vi}$	92.3(3)	$O(2)^{vi}$—Cu—Cl	95.3(2)
$O(3)^{iv}$—Te(2)—$O(3)^{iii}$	83.6(3)	$O(2)^{vii}$—Cu—Cl	173.0(2)
$O(2)^{v}$—Te(2)—$O(3)^{iii}$	71.4(3)	$O(3)^{v}$—Cu—$O(2)^{iii}$	104.8(3)
$O(1)^{vi}$—Te(2)—$O(3)^{iii}$	162.0(3)	$O(2)^{vi}$—Cu—$O(2)^{iii}$	74.6(3)
		$O(2)^{vii}$—Cu—$O(2)^{iii}$	77.9(3)
		Cl—Cu—$O(2)^{iii}$	109.09(17)

2.88 Å, however the oxygen atom O(1) is not considered to belong to the primary coordination sphere of Te(2) according to the bond valence sum calculations[31,32]. The coordination polyhedron with three short Te – O and one longer distance is common for Te^{4+} (Ref. 33). The coordinated atoms form a $[Te(2)O_{3+1}E]$ trigonal bipyramid when also the stereochemically active $5s^2$ lone pair (designated E) located in the equatorial plane is taken into account. Four $[Te(2)O_{3+1}E]$ polyhedra are connected sharing common corners to form $[Te_4O_{12}E_4]$ rings, see Figure 1a. The Te(1) atom is coordinated by four O(1) atoms to form a $[TeO_4]$ pyramid, see Figure 1b. This is a very uncommon coordination polyhedron for Te^{4+} and to our best knowledge has not been observed before. When the stereochemically active lone pair is also taken into consideration the coordinated atoms form a $[Te(1)O_4E]$ square pyramid. The Te(1) – O bonding distance is 1.987 Å and the O(1) – Te(1) – O(1) angles amount to $79.69(18)^o$. This type of coordination has previously been observed for Sb^{3+}, and Bi^{3+} in, *e.g.* in the compounds $BaSbO_2Cl$ (Ref. 35), $DyBi_2O_4I$ (Ref. 36).

The Cu atom is coordinated by four oxygen atoms and one chlorine atom to form a distorted $[CuO_4Cl]$ square pyramid. Three Cu – O bonding distances are in the range 1.911 – 2.014 Å and one long is present at 2.501 Å. The Cu – Cl bond distance is 2.244 Å. These coordinations leads to a Cu bond valence sum of +2.06 (see Table II). Each Cl atom forms only one bond that leads to voids in the structure along [001] where the Cl atoms and the Te(1) lone pair are located. Therefore the bond valence sum for the Cl^- ion in Cu-45124 is only 0.52 suggesting that it takes the role of a counter ion instead of being fully integrated in the covalent/ionic network.

Groups of four $[CuO_4Cl]$ square pyramids are connected via edge sharing to form $[Cu_4O_8Cl_4]$ units. These units are arranged such that they form tetrahedral clusters of Cu^{2+} ions (Figure 2). The $[Cu_4O_8Cl_4]$ groups are separated from each other by $[Te(2)_4O_{12}E_4]$ rings in the [001] direction and by $[Te(1)O_4E]$ square pyramids in the [100] and [010] directions. An overview of the crystal structure is given in Figure 3.

IV. COMPARISON WITH THE CRYSTAL STRUCTURE OF $Cu-2252$

The compounds Cu-2252 and Cu-45124 both crystallize in the tetragonal system but differ in space groups; *P-4* and *P4/n*, respectively. This implies that Cu-45124 is centrosymmetric. Nevertheless, the crystal structures of the

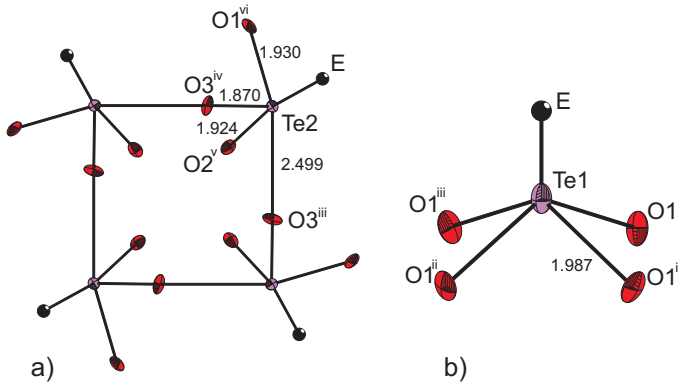

FIG. 1: (Color online) a) Four [Te(2)O_{3+1}E] polyhedra are connected via corner sharing to form [$Te_4O_{12}E_4$] rings. b) The Te(1) atom is coordinated by four O(1) atoms and the lone-pair to form a [TeO_4E] square pyramid. Distances from Te to the different oxygen are given in Å.

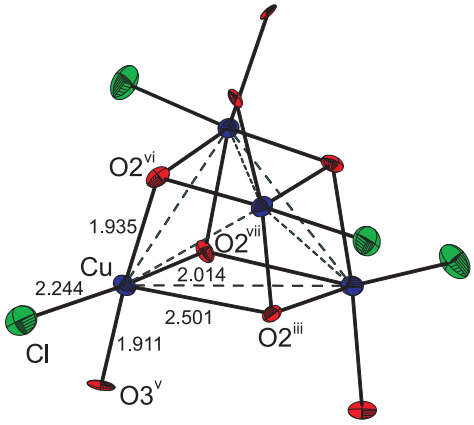

FIG. 2: (Color online) Groups of four [CuO_4Cl] square pyramids are connected via edge sharing to form [$Cu_4O_8Cl_4$] units. The Cu^{2+} ions form a distorted tetrahedron marked with dashed lines.

two compounds have many similarities. They both contain clusters of Cu(II) ions as [CuO_4Cl] square pyramids with similar bond distances and bond angles are connected to form [$Cu_4O_8Cl_4$] units. The [TeO_{3+1}] coordination around the Te atom in Cu-2252 is very similar to the coordination around Te(2) in Cu-45124.

The main difference to Cu-2252 is thus the presence of [Te(1)O_4] units in Cu-45124. These units increase the separation of the tetrahedra within the *ab* plane. Furthermore, they compress a 4-chlorine coordination to a ring which connects the tetrahedra within the *ab* plane. Thereby, Cl_4 and [Te(1)O_4] units alternate in Cu-45124 along the *c* axis. In Cu-2252 the corresponding space is filled up only by tetrahedral Cl_4. The *ab* plane projection of the crystal structure given in Figure 4 shows this arrangement in detail. Connected with this difference of stacking is a different orientation of the Cu-tetrahedra along [001]. For Cu-2252 there is one orientation while there are two different rows of Cu-tetrahedra in Cu-45124 (see Figure 5). This leads to the space groups being different for the two compounds.

A band structure study on Cu-2252 with a consequent downfolding and tight binding analysis has identified the four chlorine sites as the center controlling the in-plane inter-tetrahedra coupling. The respective hopping matrix element t_d is even comparable with the intra-tetrahedra hopping t_1[37]. We expect for Cu-45124 an elongation of the corresponding hopping paths. The in-plane magnetic exchange should then be reduced compared to the out-of-plane paths and the intra-tetrahedra exchange. This is also evident from comparing the inter- and intra tetrahedra Cu – Cu distances given in Table IV. The shortest inter-tetrahedra distance is elongated by 22% with respect to Cu-2252, X=Cl.

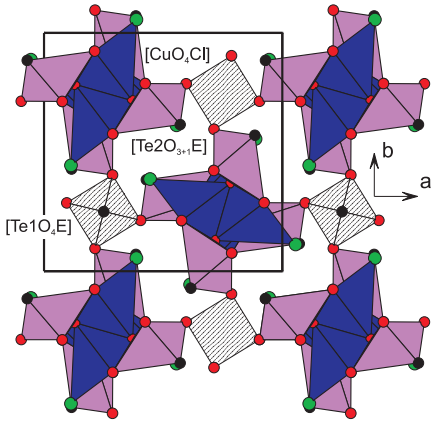

FIG. 3: (Color online) An overview of the crystal structure along [001].

TABLE IV: Intra- and shortest inter-tetrahedra Cu – Cu distances.

Compound	$\mathbf{Cu_4Te_5O_{12}Cl_4}$	$\mathbf{Cu_2Te_2O_5Cl_2}$	$\mathbf{Cu_2Te_2O_5Br_2}$
intra-tetrahedra	3.147 Å	3.229 Å	3.196 Å
	3.523 Å	3.591 Å	3.543 Å
inter-tetrahedra	5.063 Å	4.164 Å	4.39 Å

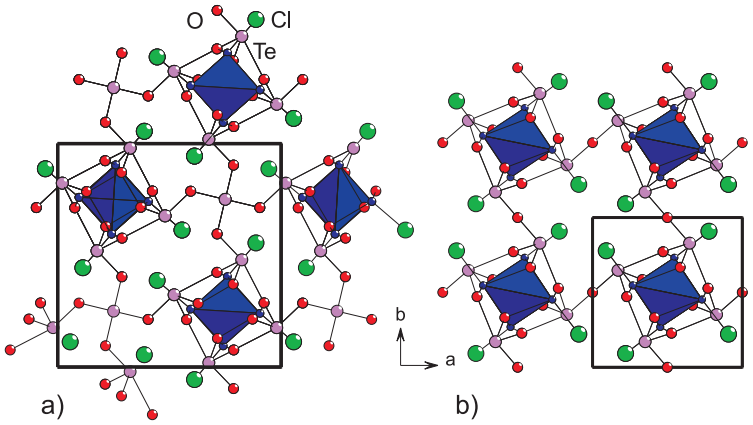

FIG. 4: (Color online) Crystal structure of a) Cu-45124 and b) Cu-2252 projected along [001]. The unit cell is outlined by the thin line. The figures scale to each other. The structures differ by the existence of an additional [Te(1)O_4] group in the center of the tetrahedra plotted for Cu-45124.

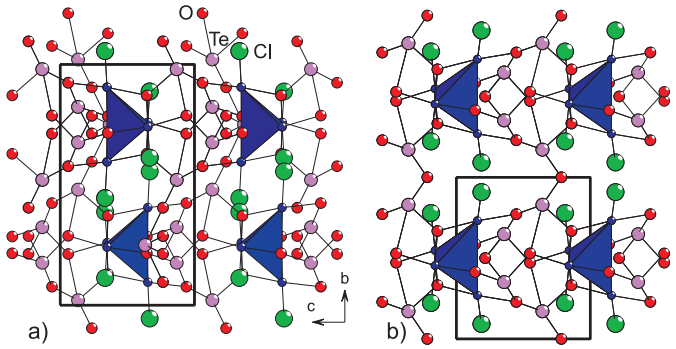

FIG. 5: (Color online) Crystal structure in *bc* plane projection of a) Cu-45124 and b) Cu-2252. The figures scale to each other.

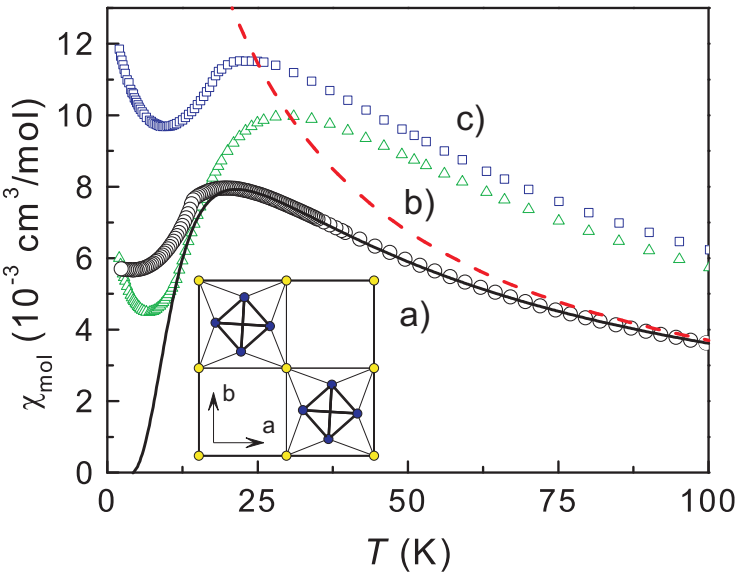

FIG. 6: (Color online) Magnetic susceptibility in a field of B=1 Tesla of a) Cu-45124, b) Cu-2251 with X=Br and c) with X=Cl, respectively[15]. The solid (dashed) curves give a fit using the isolated tetrahedron model (the high temperature Curie-Weiss behavior) described in the text. The insert shows a projection on the Cu tetrahedra (full circles) within a unit cell and the inversion centers (open circles) in Cu-45124.

V. MAGNETIC SUSCEPTIBILITY AND SPECIFIC HEAT

At high temperatures the magnetic susceptibility of Cu-45124 shows a Curie-Weiss behavior that extrapolates to a paramagnetic Curie-Weiss temperature θ_{CW} ≈-11(1) K (dashed curve in Fig. 6 and the lower inset of Fig. 7). The slope of the reciprocal susceptibility corresponds to an effective magnetic moment of 1.81(1) μ_{Bohr} per Cu^{2+} ion. With the magnetic moment arising from Cu^{2+} with S=1/2 the effective moment indicates an gyromagnetic ratio g ≈2.1, in fair agreement with the expectation for a $3d^9$ configuration. The paramagnetic Curie-Weiss temperature θ of Cu-45124 is smaller compared to Cu-2252, with X=Cl (θ_{CW} ≈-25 K). It should be highlighted that this value corresponds to a weighted sum of all inter- and intra-tetrahedra coupling constants.

The built-up of short range antiferromagnetic correlations appears in Cu-45124 for temperatures below about 80 K. This is evident as a deviation from the Curie-Weiss behavior (dashed curve in Fig. 6). Moreover, the correlations are captured rather well in a model of independent tetrahedra, with two exchange coupling constants, J_1 and J_2 which has been detailed in Ref. 14. This is evident from the solid line in Fig. 6 which represents a fit to χ_{mol} using J_1=32.9 K and J_2=18.4 K. For Cu-2252 fits of similar quality have been established with J_1=J_2=38.5 K (43K) for X=Cl (Br)[14].

At low temperature the susceptibility shows a broad maximum at T_{max}=29 K and a kink below ≈14K identified with long range ordering. There is no indication for a thermal hysteresis when comparing the field-cooled and zero-field-cooled measurement. Taking the derivative with respect to temperature[38] of the product $\chi_{mol} \cdot T$ the kink shows up as a λ-type anomaly at T_c similar to that observed in the heat capacity as shown in Figure 7. The quantity $d/dT(\chi_{mol} \cdot T)$ falls off with a long tail indicating substantial short-range antiferromagnetic correlations toward higher temperatures. The specific heat plotted in the upper part of Fig. 7 can be used to determine the magnetic entropy $S_{mag}(T)$ after subtracting an estimated lattice contribution. S(14K) contains an essential fraction of the magnetic entropy released in the phase transition and amounts to about 40 % of R·ln2, expected for a S=1/2 system. This value is a little bit larger than for Cu-2252 with X=Cl.

Characteristic temperatures and energy scales are given in Table V and compared with the data from Cu-2252. Although the overall magnetic behavior is very similar, Cu-45124 behaves more close to the corresponding chlorine Cu-2252 (X=Cl). We can use the maximum in the susceptibility to test or establish some scaling. It is evident from a comparison of T_c/T_{max} for different compounds that the composition and the related changes of the inter-tetrahedral coupling mainly effect the transition temperature T_c. The entropy at the transition determined from specific heat and the ordered moment from neutron scattering follow roughly the behavior of T_c/T_{max}. In contrast, T_{max} itself and the maximum in the magnetic Raman scattering E_m, discussed further below, are dominated by intra-tetrahedra couplings and show no obvious scaling.

The magnetic susceptibility of Cu-45124 differs from the other two Cu-2252 systems in the sense that there is no upturn at low temperatures. This also corresponds to a different low-temperature curvature. Such an upturn can

TABLE V: Data derived from magnetic susceptibility (T_c, T_{max}), specific heat (entropy $S(T_c)$) and Raman scattering (E_m, ΔE) compared with data for the other tetrahedron systems derived from Ref. 15,19,39. The ordered magnetic moment $\mu_{ord.}/\mu_B$ determined by neutron scattering is from Ref. 17,20. For X=Br the parameter ΔE corresponds to the FWHM of the continuum. Further details see text.

Compound	$Cu_2Te_2O_5Cl_2$	$Cu_4Te_5O_{12}Cl_4$	$Cu_2Te_2O_5Br_2$
T_{max}/K	23	19	30
T_c/K	18.2	13.6	11.4
T_c/T_{max}	0.79	0.72	0.38
$S(T_c)/(R{\cdot}ln2)$	0.36	0.4	0.16
$\mu_{ord.}/\mu_B$	0.7-0.9	-	0.4
E_m/cm^{-1}	47.5	36.9	60
$\Delta E/cm^{-1}$	9.0	4.7	22
E_m/T_c	3.8	3.9	7.6
E_m/T_{max}	3.0	2.8	2.9

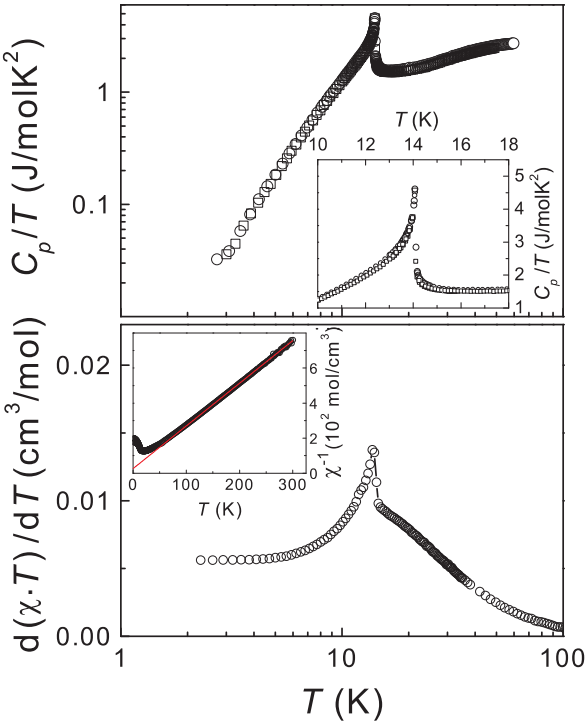

FIG. 7: (upper panel)Specific heat C_p/T of Cu-45124. The inset zooms into the transition regime. (lower panel) $d/dT(\chi_{mol}\cdot T)$ as function of temperature. The inset shows the reciprocal magnetic susceptibility.

have intrinsic or extrinsic origins. Defects may induce paramagnetic centers that show up in the susceptibility as an additional low temperature contribution with a Curie-Weiss-like temperature dependence[40,41,42]. As the discussed compounds have very similar chemical properties and are prepared from the same starting materials via very similar preparation routes, however, there is no reason to assume a fundamental different defect density. As a possible reason we suggest the existence of an inversion center and the higher symmetry of Cu-45124[43]. The inset in Figure 6 shows a projection on the unit cell including the Cu tetrahedra and respective inversion centers. Exchange paths that are inversion symmetric do not allow antisymmetric spin-spin interactions, as the DM interaction. Therefore, staggered fields[44] and effective ferromagnetic moments at low temperatures are suppressed. In $Sr_2V_3O_9$ and $Ba_2V_3O_9$ low temperature upturns in the magnetic susceptibility have been attributed to low symmetry exchange paths[45]. We are aware that this argument might only be relevant for inter-tetrahedra exchange and is qualitative as it cannot be proven for all possible exchange paths individually. However, DM interactions that are allowed for Cu-2252 have been shown to be of relevance for the stabilization of ground states with small ordered moments[13,39].

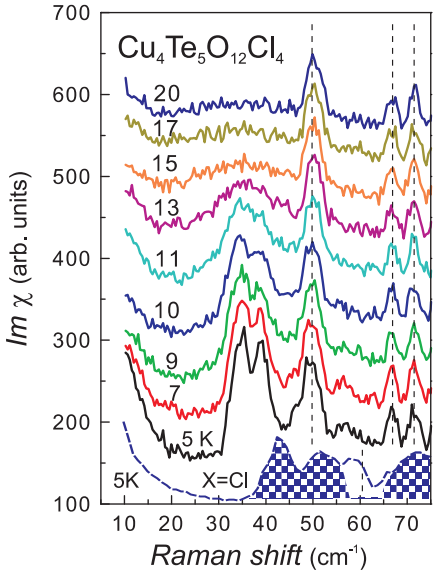

FIG. 8: (Color online) Bose corrected Raman scattering intensity of Cu-45124 at small energies and low temperatures. Phonon modes are marked by dashed lines. The curves have been given a vertical offset for clarity. The curve at the bottom corresponds to Cu-2252 with X=Cl. The three shaded maxima are the magnetic Raman intensity. A phonon with an asymmetric Fano lineshape is omitted.

VI. RAMAN SCATTERING

The overall Raman scattering intensity in Cu-45124 is very large, compared to transition metal oxides[46]. This is based on the enormous electronic polarizability and nonlinearity of oxo-tellurides that makes them promising materials for photorefractive, acousto-optical or applications related to second harmonic generation[47]. Due to the inversion center, however, photorefractive effects are not allowed in Cu-45124. Also certain phonon-phonon and spin-phonon scattering terms are forbidden. Furthermore, possible nonlinearities do not break symmetry selection rules and there exist no further evidence for a structural or electronic instability as will be shown below.

We observe 46 sharp modes in the frequency regime 40 – 800 cm^{-1} that do not show a strong or anomalous temperature dependence. Therefore they are attributed to optical phonon modes. In contrast, the low energy regime exhibits modes with frequencies of 30 – 65 cm^{-1} that evolve in the low temperature regime where the susceptibility changes, see Figure 8.

Based on the crystallographic coordinates given in Table II a symmetry analysis leads to Γ^{8g}=(3Ag +3Au+3Bg+3Bu+3Eg+3Eu) modes for each of the 6 *8g* sites and Γ^{2c}=Ag+Au+Eg+Eu modes for the *2c* site. In total Γ_{even}=58 modes are Raman active. This number is in reasonable agreement with the observed 46 modes keeping in mind that due to a near degeneracy or small intensity a few modes can be covered. In Figure 9b) the result of a temperature analysis of representative phonons is shown. The transition does not show up in the phonons, i.e. there is no evidence for pronounced spin-phonon coupling. The same observation has been made for Cu-2215 using Raman and IR spectroscopy[15,48]. It disagrees with conclusions drawn from thermal conductivity measurements on the latter compound[49].

At small Raman shifts there are two modes (34.5 cm^{-1}, 39.2 cm^{-1}) that show a pronounced temperature dependence of the intensity close to T_c and one weaker maximum (58 cm^{-1}), see Figure 8. The analysis of this data is given in Figure 9a). The main modes develop from a very broad maximum that gradually shifts to higher energy and then splits-up equidistantly right at the transition. In the same temperature regime the linewidth of the modes strongly decreases. We do not observe quasielastic scattering at elevated temperatures that is common for low dimensional spin systems[46]. In contrast, a tiny increase of intensity is seen at lowest temperatures. We attribute these modes to magnetic scattering as their energy and temperature dependence match the related energy scales. The bottom curve in Figure 8 shows the corresponding data for Cu-2252 with X=Cl. There are two similar maxima at 43 and 52 cm^{-1}, a phonon at ≈60 cm^{-1} and a third magnetic mode at 73 cm^{-1}.

To characterize the magnetic scattering on a molecular field like level we determine the mean frequency E_m=36.9 cm^{-1} and the splitting of the modes ΔE=4.7 cm^{-1} for Cu-45124. It is obvious from Figure 9 that E_m, characteristic for a magnetic energy scale, is only weakly temperature dependent. In contrast, ΔE, increases rapidly at $T=T_c$ and is constant to lower temperatures. The temperature dependence is even sharper than expected for a

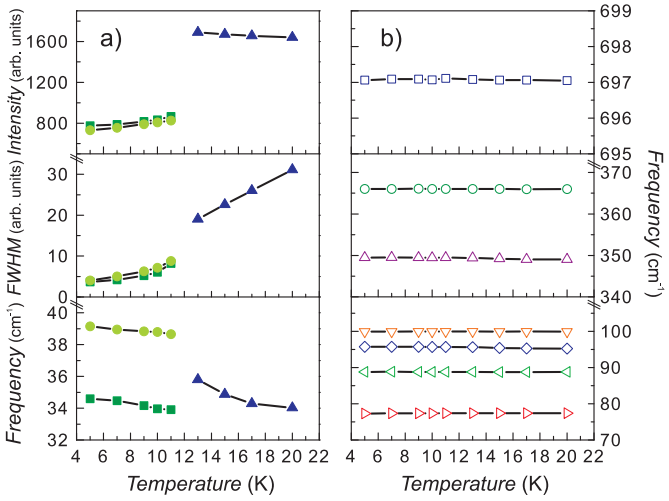

FIG. 9: (Color online) Analysis of the temperature dependence of the a) low energy modes and b) phonon modes in Raman scattering.

magnetic order parameter.

VII. DISCUSSION

The ambivalence of weakly coupled spin cluster systems in the proximity to a quantum critical point is an interesting topic and it has been shown that both thermodynamic and spectroscopic tools have to be used to understand their properties[10,13,50,51]. The presently studied tetrahedra systems fall into the rare case where both local and collective excitations can be observed simultaneously, and where the character of the excitation spectrum changes with minute changes of external parameters.

In the limit of weak coupling, i.e. in the quantum disordered phase, a set of gapped low energy excitations exists with energies characteristic for the intra-tetrahedra or -dimer couplings. Such modes have been observed using different spectroscopic tools, e.g. in the frustrated dimer system $SrCu_2(BO_3)_2$[53,54,55,56,57]. In the limit of strong inter-tetrahedra and weak intra-tetrahedra coupling long range ordering leads to gapless collective modes. In Raman scattering such modes are observed as broadened two-particle continua with energies up to a few times the coupling constant. Such a scattering contribution survives elevated temperatures with respect to its integrated intensity. However, it softens considerably to lower energies and forms quasi-elastic tails. Theoretical modeling of two-particle Raman scattering on spin tetrahedra systems showed symmetric continua only if the inter-tetrahedra couplings do not dominate, e.g. due to a coupling to chains of tetrahedra[10,11,52]. In such models the determination of a mean energy of the continuum E_m is meaningful as its position is mainly determined by the strong intra-tetrahedra couplings.

This allows us to derive a correspondence between the Raman data and other parameters of the systems. The bottom of Table V shows a synopsis for all tetrahedra systems[16,39,58]. In Cu-2252 with X=Br the broad, symmetrical continuum leads to a very large E_m=60 cm^{-1}. From a comparison with the other systems it is clear that this parameter scales with the maximum position in the susceptibility. We attribute changes of E_m to modulations of the intra-tetrahedra coupling. Only for Cu-2252 with X=Br, the system with the smallest inter-tetrahedra coupling, the strongly reduced ordered moment shows longitudinal fluctuations[59,60] observed as a distinct longitudinal magnon mode at 18 cm^{-1} (Refs. 18 and 39). The energy separation of the continuum to this mode is of the order of the intra tetrahedra coupling[15,18] and should be an indication for the proximity to a quantum critical point.

In contrast, Cu-2252 with X=Cl and even more Cu-45124 show splittings with considerably smaller energies ΔE. We propose two-spin anisotropies to be responsible for these effects as the weaker inter-tetrahedra coupling should lead to broader signals and single ion anisotropies do not exist for Cu^{2+} with s=1/2. Including DM interaction into the Hamiltonian of $SrCu_2(BO_3)_2$ a very satisfactory description of Raman modes and splittings of ESR lines have been accomplished[57]. For Cu-2252 with X=Br the field dependence of the longitudinal magnon and T_c has been modeled[39]. Within this approach we would expect a smaller contribution of the DM interaction as the normalized splitting is $\Delta E/E_m$=12.7 for Cu-45124 compared to $\Delta E/E_m$=19 for Cu-2252 with X=Cl. This is consistent with the behavior of the low temperature susceptibility.

The structural difference between the compounds discussed in Chapter IV are summarized as a reduction of the

inplane inter-tetrahedra coupling introducing additional [Te(1)O_4] groups. The different stacking of the tetrahedra and the inversion center are expected to affect the out-of-plane exchange, however, only to a minor degree. The question remains which scenario dominates the spin fluctuations in Cu-45124 irrespective of the exact ground state. Is the dimensionality enhanced by a decreasing in-plane exchange with respect to out-of-plane exchange? As a result the character of the transition should be more mean field-like. Or does the same reduction of the in-plane exchange enhances the effect of frustration of the intra tetrahedra exchange? Although in Cu-45124 the small number of low energy excitations might be taken as evidence for competing interactions, the reduced transition temperature while keeping the entropy constant proposes that the change of dimensionality is more effective for Cu-45124. Noticeably, recent *ab initio* calculations on this new tellurate compound support the mean field nature of the magnetic behavior as observed experimentally[61].

Neutron scattering experiments on Cu-2252 show that a complex helical state with a reduced ordered moment can be used to describe the ordered state[17,20]. Inelastic scattering detects two kind of excitations, a dispersionless high energy mode at $\approx$48 cm^{-1} and a dispersing mode with a gap of $\approx$16 cm^{-1}. Remarkably, for X=Cl the dispersionless mode survives to elevated temperatures and is only moderately depressed for T>T_c[63]. These observations support our results and we expect a similar trend for Cu-45124. Further Raman scattering and thermodynamic experiments are prepared to test whether controlled substitutions or pressure can be used to shift Cu-45124 more closer to the quantum critical point similar to observations in Cu-2252[16,21].

VIII. CONCLUSIONS

The compound Cu-45124 has been established as the second example of a system with weakly interacting s=1/2 spin tetrahedra. Results from Raman scattering and thermodynamic experiments have been compared with the related compounds and discussed in terms of simple scaling arguments. We conclude a reduced effect of competing interactions and a mean field like behavior in the present system compared to the intensively investigated system Cu-2252.

IX. ACKNOWLEDGEMENTS

This work has been carried out with financial support from the Swedish Research Council, the German Science Foundation and the ESF program *Highly Frustrated Magnetism*. We acknowledge important discussions with R. Valentí.

[1] E. Dagotto, *Phase Separation and Collossal Magnetoresitance*, (Berlin: Springer) 2002.
[2] P. W. Anderson, Solid State Phys. **14**, 99 (1963).
[3] F. Mila, Eur. J. Phys. **21**, 499 (2000).
[4] J. E. Greedan, J. Mater. Chem. **11**, 37 (2001).
[5] C. Lhuillier, Lecture notes (fall 2002) "Ecole de troisieme cycle de Suisse Romande", cond-mat/0502464 (2005).
[6] A. P. Ramirez, A. Hayashi, R. J. Cava, R. Siddharthan, and B. S. Shastry, Nature **399**, 333 (1999).
[7] A. T. Bramwell and M. J. P. Gingras, Science **294**, 1495 (2001).
[8] S.-H. Lee, C. Broholm, W. Ratcliff, G. Gasparovic, Q. Huang, T. H. Kim, and S.-W. Cheong, Nature **418**, 856 (2002).
[9] S. H. Lee, D. Louca, H. Ueda, S. Park, T. J. Sato, M. Isobe, Y. Ueda, S. Rosenkranz, P. Zschack, J. Iniguez, Y. Qiu, , and R. Osborn, Phys. Rev. Lett **93**, 156407 (2004).
[10] W. Brenig and K. W. Becker, Phys. Rev. B **64**, 214413 (2001).
[11] W. Brenig, Phys. Rev. **B 67**, 064402 (2003).
[12] W. Brenig and M. Grzeschik, Phys. Rev. **B 69**, 064420 (2004).
[13] V. N. Kotov, M. E. Zhitomirsky, M. Elhajal, and F. Mila, Phys. Rev. **B 70**, 214401 (2004).
[14] M. Johnsson, K. W. Törnroos, F. Mila, and P. Millet, Chem. Mater. **12**, 2853 (2000).
[15] P. Lemmens, K.-Y. Choi, E. E. Kaul, C. Geibel, K. Becker, W. Brenig, R. Valentí, C. Gros, M. Johnsson, P. Millet, and F. Mila, Phys. Rev. Lett. **87**, 227201 (2001).
[16] P. Lemmens, K.-Y. Choi, G. Güntherodt, M. Johnsson, P. Millet, F. Mila, R. Valentí, C. Gros, and W. Brenig, Physica **B 329-333**, 1049 (2003).
[17] O. Zaharko, A. Daoud-Aladine, S. Streule, J. Mesot, P.-J. Brown, and H. Berger, Phys. Rev. Lett. **93**, 217206 (2004).
[18] C. Gros, P. Lemmens, M. Vojta, R. Valentí, K. Y. Choi, H. Kageyama, Z. Hiroi, N. Mushnikov, T. Goto, M. Johnsson, and P. Millet, Phys. Rev. **B 67**, 174405 (2003).

[19] P. Lemmens, K.-Y. Choi, A. Ionescu, J. Pommer, G. Güntherodt, R. Valentí C. Gros, W. Brenig, M. Johnsson, P. Millet, and F. Mila, Journ. Phys. Chem. Solids **63/6-8**, 1115 (2002).
[20] O. Zaharko, H. M. Ronnow, A. Daoud-Aladine, S. Streule, F. Juranyi, J. Mesot, H. Berger, and P.-J. Brown, Physika Nizkikh Temperatur **31**, N8/9 (2005) (cond-mat/0502165).
[21] J. Kreitlow, S. Süllow, D. Menzel, J. Schoenes, P. Lemmens, and M. Johnsson, Journ. Magn. Mag. Mater. **290**, 959 (2005).
[22] S. J. Crowe, M. R. Lees, D. McK. Paul, R. I. Bewley, J. W. Taylor, G. McIntyre, O. Zaharko, and H. Berger, cond-mat/0601023 (2006).
[23] X. Wang, I. Loa, K. Syassen, P. Lemmens, M. Hanfland, and M Johnsson, J. Phys.: Cond. Matter **17**, 807 (2005).
[24] R. Valentí, T. Saha-Dasgupta, C. Gros, and H. Rosner, Phys. Rev. **B 67**, 245110 (2003).
[25] R. Becker, M. Johnsson, R. K. Kremer, and P. Lemmens, Journ. Solid State Chem. **178**, 2024 (2005).
[26] X-SHAPE revision 1.06, STOE & Cie GmbH, Darmstadt, Germany (1999).
[27] X-RED version 1.22, STOE & Cie GmbH, Darmstadt, Germany (2001).
[28] G. M. Sheldrick, SHELXS97, Program for solution of crystal structures, Göttingen, Germany (1997).
[29] G. M. Sheldrick, SHELXL97, Program for refinement of crystal structures, Göttingen, Germany (1997).
[30] Supplementary crystallographic material has been sent to Fachinformationzentrum Karlsruhe, Abt. PROKA, 76344 Eggenstein-Leopoldshafen, Germany (fax +49-7247-808-666; E-mail: crysdata@fiz-karlsruhe.de), and can be obtained on quoting the deposit number CSD-415538.
[31] I. D. Brown and D. Altermatt, Acta Cryst. **B 41**, 244 (1985).
[32] I. D. Brown, *The Chemical Bond in Inorganic Chemistry – The Bond Valence Model* (Oxford university press, Oxford, 2002).
[33] J. Zemann, Monatshefte für Chemie **102**, 1209 (1971).
[34] N. Brese and M. O'Keeffe, Acta Cryst. **B 47**, 192 (1991).
[35] F. Thuillier-Chevin, P. Maraine, and G. Perez, Revue de Chimie Minerale **17**, 102 (1980).
[36] M. Schmidt, H. Oppermann, C. Hennig, R. Henn, E. Gmelin, N. Soeger, and M. Binnewies, Zeitschrift für Anorg. und Allg. Chemie **626**, 125 (2000).
[37] T. Saha-Dasgupta, R. Valentí, H. Rosner, and C. Gros, Europhys. Lett. **67**, 63 (2004).
[38] R. K. Kremer and J. E. Greedan, J. Solid State Chem. **73**, 579 (1988) and references therein.
[39] J. Jensen, P. Lemmens, and C. Gros, Europhys. Lett. **64**, 689 (2003).
[40] M. Laukamp, G. B. Martins, C. Gazza, A. L. Malvezzi, E. Dagotto, P. M. Hansen, A. C. Lopez, and J. Riera, Phys. Rev. B **57**, 10755 (1998).
[41] M. Fischer, P. H. M. van Loosdrecht, P. Lemmens, G. Güntherodt, B. Büchner, T. Lorenz, M. Breuer, J. Zeman, G. Martinez, G. Dhalenne, and A. Revcolevschi, Phys. Rev. B **57**, 7749 (1998).
[42] K. Manabe, H. Ishimoto, N. Koide, Y. Sasago, and K. Uchinokura, Phys. Rev. B **58**, R575 (1998).
[43] The inversion centers at (1/2, 1/2, 1/2), also present at (1/2, 0, 1/2) and at (0, 1/2, 1/2) due to symmetry operations, connect tetrahedra. They affects the symmetry of intra-tetrahedra exchange.
[44] I. Affleck and M. Oshikawa, Phys. Rev. B **60**, 1038 (1999).
[45] E. E. Kaul, H. Rosner, V. Yushankhai, J. Sichelschmidt, R. V. Shpanchenko, and C. Geibel, Phys. Rev. **B 67**, 174417 (2003).
[46] P. Lemmens, G. Güntherodt, and C. Gros, Physics Reports **375**, 1 (2003).
[47] K. V. Domoratskii, V. I. Pastukhov, A. Y. Kudzin, L. Y. S. V. M. Rizak, and V. A. Stefanovich, Physics of the Solid State **42**, 1443 (2000).
[48] A. Perucchi, L. Degiorgi, H. Berger, and P. Millet, Eur. Phys. J. **B 38**, 65 (2004).
[49] M. Prester, A. Smontara, I. Zivkovic, A. Bilusic, D. Drobac, H. Berger, and F. Bussy, Phys. Rev. **B 69**, 180401 (2004).
[50] V. N. Kotov, O. P. Sushkov, and R. Eder, Phys. Rev. B **59**, 6266 (1999).
[51] V. N. Kotov, M. E. Zhitomirsky, and O. P. Sushkov, Phys. Rev. B **63**, 64412 (2001).
[52] W. Brenig, K. W. Becker, and P. Lemmens, Physica **B 312**, 594 (2002).
[53] H. Kageyama, M. Nishi, N. Aso, K. Onizuka, T. Yoshihama, K. Nukui, K. Kodama, K. Kakurai, and Y. Ueda, Phys. Rev. Lett. **84**, 5876 (2000).
[54] P. Lemmens, M. Grove, M. Fischer, G. Güntherodt, V. N. Kotov, H. Kageyama, K. Onizuka, and Y. Ueda, Phys. Rev. Lett. **85**, 2605 (2000).
[55] H. Nojiri, H. Kageyama, Y. Ueda, and M. Motokawa, J. Phys. Soc. Jpn. **72**, 3243 (2003).
[56] N. Aso, H. Kageyama, K. Nukui, M. Nishi, H. Kadowaki, Y. Ueda, and K. Kakurai, Journ. of the Phys. Soc. Jpn. **74**, 2189 (2005).
[57] A. Gozar, B. S. Dennis, H. Kageyama, and G. Blumberg, Phys. Rev. **B 72**, 064405 (2005).
[58] K.-Y. Choi, P. Lemmens, H. Berger, et al., in preparation (2005).
[59] Z. Tun, W. J. L. Buyers, R. L. Armstrong, K. Hirakawa, and B. Briat, Phys. Rev. B **42**, 4677 (1990).
[60] A. Zheludev, M. Kenzelmann, S. Raymond, T. Masuda, K. Uchinokura, and S.-H. Lee, Phys. Rev. B **65**, 014402 (2002).
[61] B. Rahaman, R. Valentí, T. Saha-Dasgupta, to be published (2006).
[62] S. J. Crowe, S. Majumdar, M. R. Lees, D. McK. Paul, S. J. Levett, and C. Ritter, Phys. Rev. B **71**, 224430 (2005).
[63] S. Streule, pers. communication (2005), and S. Streule, H. M. Ronnow, Ch. Niedermayer, H. Berger, J. Mesot, SINQ progress report (2005).